Reduced-order modeling for sputtering of monoatomic materials by noble gas bombardment

IEPC-2025-090

Presented at the 39th International Electric Propulsion Conference Imperial College London • London, United Kingdom 14-19 September 2025

Anthony Kim¹ and Huy Tran²
University of Illinois Urbana-Champaign, Urbana, IL, 61801, USA
Argonne National Laboratory, Lemont, IL, 60439, USA

Huck Beng Chew³
University of Illinois Urbana-Champaign, Urbana, IL, 61801, USA

Abstract: The lifetime of electric space propulsion systems is controlled by the sputtering of critical plasma-facing components by noble gas ion bombardment, since ion-induced sputtering causes surface erosion, reshapes the surface topography unexpectedly, and degrades the electric propulsion system. Elucidating the erosion rate of these critical components requires an accurate assessment of the sputtering yield. In this work, we utilize molecular dynamics (MD) simulations to obtain sputtering yield data for iron (Fe), Zirconium (Zr), Aluminum (Al), and Silver (Ag). We also propose a two-parameter sputtering yield model that requires two sputtering datapoints – the sputtering threshold energy and the saturated ion energy – to predict the evolution of sputtering yield versus ion energy for the different ion/target combinations. We conclude that our MD simulation results and reduced-order sputtering yield model show good agreement with available experimental results.

Nomenclature

 θ = incidence angle α = azimuthal angle a_{lat} = lattice parameter

 E_c = critical energy of sputtering yield saturation

 Y_c = critical sputtering yield

 E_{th} = threshold energy for sputtering

 a_{lat} = lattice parameter

I. Introduction

In thrusters have been designed for miscellaneous space missions. The ion thruster is a type of electric propulsion system that generates thrust by ionizing neutral gas (typically Xenon) and then accelerating the resulting positive ions to extremely high speeds using electric or magnetic fields. The advantage of ion thrusters is that they have high

³ Professor, Aerospace Engineering, hbchew@illinois.edu



The 39th International Electric Propulsion Conference, Imperial College London, London, United Kingdom 14-19 September 2025

Page 1

¹ PhD student, Aerospace Engineering, ak131@illiois.edu

² Postdoctoral Researcher, Argonne National Laboratory, tranh@anl.gov

specific impulses (the ratio of thrust to the rate of propellant consumption), meaning less propellant is needed for a given mission. Ion thrusters basically consist of a neutralizer, cathode, accelerator grid, and a plasma generator (discharge chamber) [1]. The cathode emits the electrons, and the electrons collide with the neutral propellant atoms within a discharge chamber. The positive ions are directed towards the accelerator grids, and the neutralizer provides electrons to balance the charge in the thruster. Energetic ion bombardments on the acceleration grid can lead to system failure since they damage the grid surfaces by removing materials from the grid structure and enlarging holes. This phenomenon is called sputtering, which causes erosion, degradation, a reduction in operational lifespan, and structural failures.

The phenomenon of sputtering has been well-studied for over several decades, but much of the data for sputtering has been limited to high-energy (> 1 keV) sputtering. The ion energies associated with ion thruster erosion are much lower (< 1 keV). However, experimental measurements at such low ion energies are challenging because of the low sputter yield, leading to large uncertainties in the data. In addition, current semi-empirical sputtering yield models developed by Sigmund [2], Bohdansky [3], Yamamura [4], and Eckstein [5] typically have phenomenological parameters that are fitted to experimental data. Since these phenomenological parameters, to a large extent are not well-grounded in physics, it remains a challenge to extrapolate these semi-empirical models to different ion/target combinations

In this work, we conduct massively-parallel molecular dynamics (MD) simulations to obtain the sputtering yield data for the bombardment of Xe ions on Iron (Fe), Zirconium (Zr), Aluminum (Al), and Silver (Ag) substrates, under a normal ion incidence angle. We also propose a two-parameter sputtering yield model capable of predicting the entire sputtering yield versus ion energy response for different ion/target combinations. We further compare our MD simulation results and two-parameter model against existing experimental data in the literature.

II. Methodology

Molecular dynamics (MD) simulations

The classical MD simulation code, Large-scale Atomic/Molecular Massively Parallel Simulator (LAMMPS), was used to model the particles and their interactions at the atomistic scale. We simulate the repeated bombardment of Xenon (Xe) ions on Iron (Fe), Zirconium (Zr), Aluminum (Al), and Silver (Ag) substrates; each substrate is modeled to have crystalline lattice dimensions of $(20a_{lat} \times 20a_{lat} \times 60a_{lat})$ in the $(x \times y \times z)$ directions, with periodic boundary conditions assigned in the in-plane (x, y) directions. Figure 1 shows a snapshot of a sputtered Fe atom under the bombardment of Xe ions, with the incoming Xe ion marked as orange and the sputtered Fe atom marked as blue. The substrate consists of fixed layers, damping layers, heat bath layers, and free layers. These respective layers are responsible for providing structural stability, absorbing the collision effects, keeping the substrate at a constant temperature before and after each bombardment, and serving as a designated region for sputtering. The interactions between the incoming ions and the incoming ions and substrate atoms were modeled using the Ziegler-Biersack-Littmark (ZBL) potential [6], which is suitable for modeling high-energy collisions. The interactions between the substrate atoms were modeled using the Embedded Atom Method (EAM) potentials [7] from the references. For each bombardment, a single Xenon ion was deposited $5a_{lat}$ above the substrate surface at normal incidence ($\theta = 0^{\circ}$), with varying energy levels. Before the bombardment begins, the entire substrate is maintained at a target temperature of 400 K for 30 ps. The bombardment is initiated for 1 ps after the thermostat in the free layer is turned off, with a time step of 0.1 fs. Then the system is allowed to equilibrate on its own for the next 20 ps with a timestep of 1 fs. For the last step, the thermostat in the heat-bath layer is activated for the next 20 ps to quench the system, with a designated timestep of 1 fs. After each bombardment, we count the number of sputtered atoms by tracking the locations of the sputtered atoms. The above process is repeated iteratively until a total of 400 Xe ion bombardments are reached. We then obtain the sputtering yield, which is defined as the ratio of the number of sputtered atoms to the number of incoming ions. Figure 2 shows the number of sputtered atoms versus the number of bombarded ions for the Xe ion bombardment of Fe substrates following the procedure outlined here, for various ion energies. The near linearity of each slope suggests that steady-state sputtering yield is attained very soon after the initial few (< 10) ion bombardments. Each slope provides the sputtering yield of Xe ions on Fe, which is summarized in Table 1.



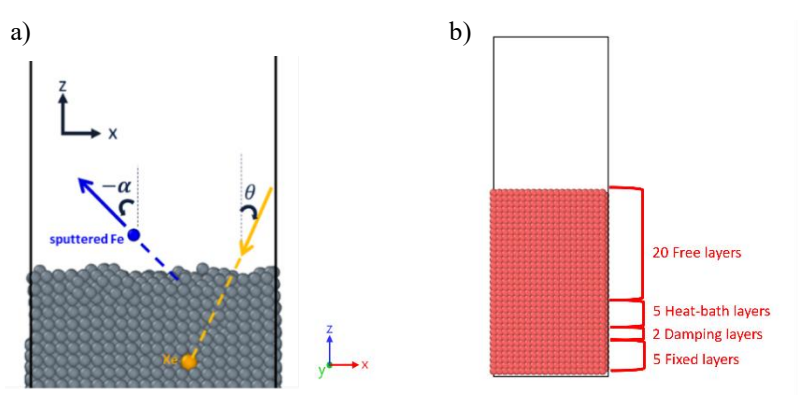


Figure 1. Snapshot of the sputtering of an iron atom under a Xe ion bombardment (a) and the modeled structure of the Iron substrate in MD simulation (b).

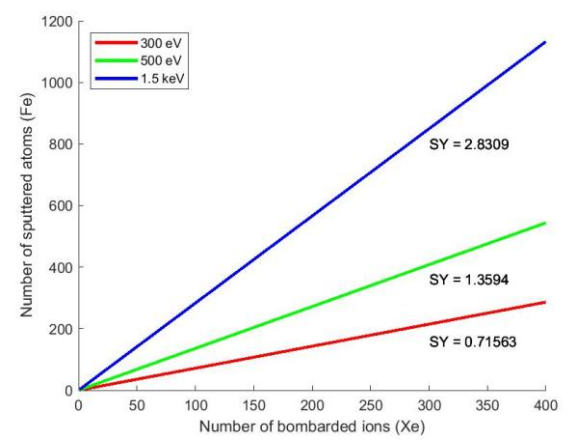


Figure 2. Number of sputtered (Iron) atoms versus total number of bombarded Xe ions and the derived sputtering yield.

Table 1. Selected ion energy levels and corresponding sputtering yield of Iron acquired from MD simulations.

Xe (eV)	Sputtering Yield (atom/ion)
300 eV	0.71563
500 eV	1.3594
1,500 eV	2.8309



III. Case study: Xenon bombardment on Iron (Fe), Zirconium (Zr), Aluminum (Al), and Silver (Ag)

A. MD simulation results

Figure 3 shows the damage zones formed by the bombardment of a single Xe ion on Al targets after 1 ps across a wide range of ion energies. A Common Neighbor Analysis (CNA) was performed to investigate the crystal structure of the substrate. The sky-blue colored atoms denote the FCC structure, and the red colored atoms indicate the displaced atoms by the incident ions. As the ion energy increases, the penetration depth increases, and the damage zone is created deep in the substrate. Also, as the ion fluence increases, more atoms are displaced from their initial positions, and more atoms in the free layer that are close to the surface become susceptible to sputtering.

Figure 4 shows the obtained MD data as a function of ion energy under the bombardment of Xenon ions on a log scale. The MD simulation results show good agreement with the experimental results from Rosenberg [8], Tartz [9], Tondu [10], Weijsenfeld [11], and Williams [12]. It is noticeable in the sputtering yield curve that above a certain energy level E_c , the sputtering yield converges to a certain sputtering yield Y_c . This is because the high-energy ions knocked out the target atoms towards the bottom of the substrate at a deeper location, making the displaced atoms difficult to sputter.

B. Proposed Sputtering Yield Models

Following our MD data, we propose two sputtering yield models that can predict the sputtering yield of various ion/target combinations, based on our ability to quantify two anchoring datapoints. The first anchoring point is designated at the start of the sputtering yield curve, i.e., at the threshold energy. Because of the difficulty of obtaining the actual threshold energy from MD simulations, we operationally define the threshold energy E_{th} at the sputter yield of 10^{-4} . We define the second anchoring (saturation) point as the critical ion energy E_c when the saturation in the sputtering yield Y_c was attained, i.e., the datapoint where both the first and second derivative of the sputtering yield Y_c is achieved.

The following are the two possible analytical models.

$$\frac{Y_{c}-Y}{Y_{c}-10^{-4}} = \left(\frac{E_{c}-E}{E_{c}-E_{th}}\right)^{3} \tag{1}$$

$$\frac{\ln Y_{c} - \ln Y}{\ln Y_{c} - \ln 10^{-4}} = \left(\frac{\ln E_{c} - \ln E}{\ln E_{c} - \ln E_{th}}\right)^{3}$$
(2)

Figure 4 shows the curve-fitted results using these two models on a log scale. The Xe/Al, Xe/Zr, and Xe/Fe data tend to follow the log third-order polynomial model, while the Xe/Ag data comply with the third-order polynomial model. The first anchoring point (E_{th} , 10^{-4}) is denoted as a yellow-green star and the second anchoring point (E_{c} , Y_{c}) is marked as a red star for each ion/target combination.



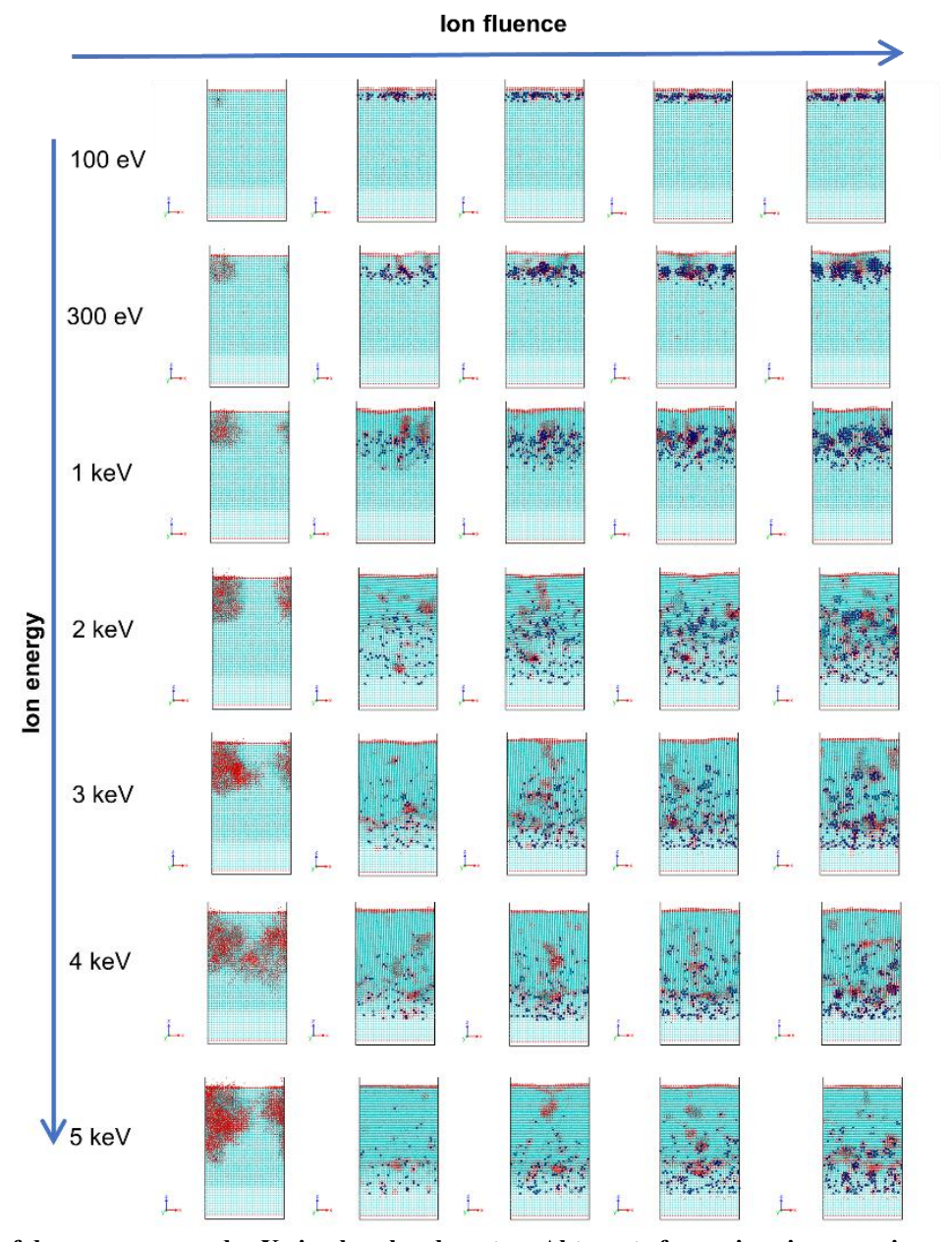


Figure 3. Formation of damage zones under Xe ion bombardment on Al targets for various ion energies, as colored by the centro-symmetry parameter: sky-blue color atoms: FCC structure, red color atoms: displaced atoms.



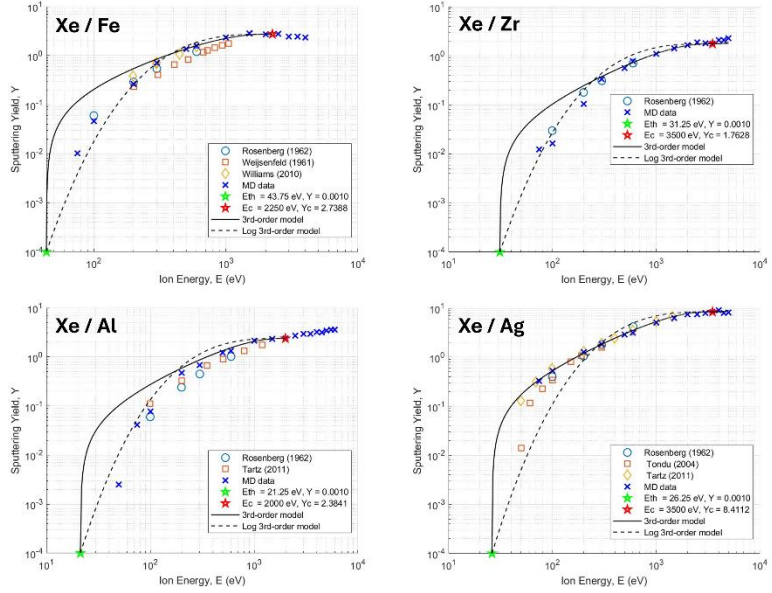


Figure 4. Sputtering yield versus ion energy from MD simulations (cross symbols), experiments (other symbols), and our two-parameter analytical models (lines).

IV. Conclusions and Future Works

In conclusion, we have obtained the MD data for the Xe ion bombardment of four different substrate materials. The number of sputtered atoms versus the incoming Xe ions exhibits a near-linear relationship, suggesting that the steady-state sputtering yield is attained almost immediately under very low fluence. More interestingly, the sputtering yield tends to saturate once the ion energy reaches a critical limit. Based on the obtained MD data, we proposed a (log) third-order polynomial model that can successfully predict the sputtering yield response of various ion/target combinations. For future work, we are planning to simulate additional noble gas ion (Xe, Kr, Ar, Ne)/target (BCC, FCC) combinations to test and verify our sputtering yield model and derive an analytic expression of E_c using the ion and target material properties by applying symbolic regression.

Acknowledgments

This work is supported by NASA through the Joint Advanced Propulsion Institute, a NASA Space Technology research Institute, grant number 80NSSC21K118. The Rosen Center for Advanced Computing (Anvil) and Texas Advanced Computing Center (TACC) are acknowledged for providing computational resources through allocations MAT 230055 and MSS22006. Also, ACCESS is highly appreciated.

References

- [1] S. E. Rahaman, A. K. Singh, S. K. Shukla, and R. K. Barik, "Analytical Modeling of Low Erosion Extraction Grid for Ion Thruster," *IEEE Trans. Plasma Sci.*, vol. 45, no. 11, pp. 2974–2978, Nov. 2017, doi: 10.1109/TPS.2017.2752260.
- [2] P. Sigmund, "Sputtering by ion bombardment theoretical concepts," in *Sputtering by Particle Bombardment I*, vol. 47, R. Behrisch, Ed., in Topics in Applied Physics, vol. 47., Berlin, Heidelberg: Springer Berlin Heidelberg, 1981, pp. 9–71. doi: 10.1007/3540105212 7.
- [3] J. Bohdansky, "A universal relation for the sputtering yield of monatomic solids at normal ion incidence," *Nuclear Instruments and Methods in Physics Research Section B: Beam Interactions with Materials and Atoms*, vol. 2, no. 1–3, pp. 587–591, Mar. 1984, doi: 10.1016/0168-583X(84)90271-4.



- [4] Y. Yamamura and H. Tawara, "ENERGY DEPENDENCE OF ION-INDUCED SPUTTERING YIELDS FROM MONATOMIC SOLIDS AT NORMAL INCIDENCE," *Atomic Data and Nuclear Data Tables*, vol. 62, no. 2, pp. 149–253, Mar. 1996, doi: 10.1006/adnd.1996.0005.
- [5] W. Eckstein and R. Preuss, "New fit formulae for the sputtering yield," *Journal of Nuclear Materials*, vol. 320, no. 3, pp. 209–213, Aug. 2003, doi: 10.1016/S0022-3115(03)00192-2.
- [6] D. A. Bromley, Ed., Treatise on Heavy-Ion Science. Boston, MA: Springer US, 1985. doi: 10.1007/978-1-4615-8103-1.
- [7] M. S. Daw and M. I. Baskes, "Embedded-atom method: Derivation and application to impurities, surfaces, and other defects in metals," *Phys. Rev. B*, vol. 29, no. 12, pp. 6443–6453, June 1984, doi: 10.1103/PhysRevB.29.6443.
- [8] D. Rosenberg and G. K. Wehner, "Sputtering Yields for Low Energy He+-, Kr+-, and Xe+-Ion Bombardment," *Journal of Applied Physics*, vol. 33, no. 5, pp. 1842–1845, May 1962, doi: 10.1063/1.1728843.
- [9] M. Tartz, T. Heyn, C. Bundesmann, C. Zimmermann, and H. Neumann, "Sputter yields of Mo, Ti, W, Al, Ag under xenon ion incidence," *Eur. Phys. J. D*, vol. 61, no. 3, pp. 587–592, Feb. 2011, doi: 10.1140/epjd/e2010-10553-8.
- [10] Tondu, T., Inguimbert, V., Darnon, F., and Roussel, J. F., "Angular characterisation of erosion and contamination by electric propulsion." 4th International Spacecraft Propulsion Conference, ESA SP-555, 2004.
- [11] C. H. Weijsenfeld, A. Hoogendoorn, and M. Koedam, "Sputtering of polycrystalline metals by inert gas ions of low energy (100–1000 eV)," *Physica*, vol. 27, no. 8, pp. 763–764, Aug. 1961, doi: 10.1016/0031-8914(61)90093-3.
- [12] Williams, J. D., Gardner, M. M., Johnson, M. L., and Wilbur, P. J., "Xenon sputter yield measurements for ion thruster materials." 28th International Electric Propulsion Conference, IEPC-2003-130,2003.

